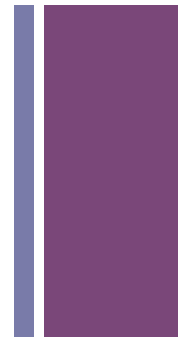


+



STAX

Paolo SPAGNOLO
INFN - Pisa



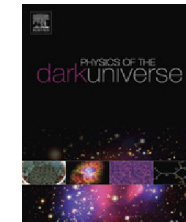
Physics of the Dark Universe 12 (2016) 37–44



Contents lists available at [ScienceDirect](#)

Physics of the Dark Universe

journal homepage: www.elsevier.com/locate/dark



Axion-like particle searches with sub-THz photons



L.M. Capparelli ^a, G. Cavoto ^b, J. Ferretti ^c, F. Giazotto ^d, A.D. Polosa ^{c,e,*}, P. Spagnolo ^f

^a Department of Physics and Astronomy, University of California Los Angeles, 475 Portola Plaza, Los Angeles, CA 90095, USA

^b INFN Sezione di Roma, P.le Aldo Moro 5, I-00185 Roma, Italy

^c Dipartimento di Fisica and INFN, 'Sapienza' Università di Roma, P.le Aldo Moro 5, I-00185 Roma, Italy

^d NEST, Istituto Nanoscienze-CNR and Scuola Normale Superiore, I-56127 Pisa, Italy

^e CERN-TH, CH-1211 Geneva 23, Switzerland

^f INFN Sezione di Pisa, Largo Bruno Pontecorvo, 3, 56127 Pisa, Italy

ARTICLE INFO

Article history:

Received 23 October 2015

Received in revised form

28 January 2016

Accepted 29 January 2016

ABSTRACT

We propose a variation, based on very low energy and extremely intense photon sources, on the well established technique of Light-Shining-through-Wall (LSW) experiments for axion-like particle searches. With radiation sources at 30 GHz, we compute that present laboratory exclusion limits on axion-like particles might be improved by at least four orders of magnitude, for masses $m_a \lesssim 0.01$ meV. This could motivate research and development programs on dedicated single-photon sub-THz detectors.

© 2016 Elsevier B.V. All rights reserved.

Keywords:

Axion-like particles

Dark-matter constituents

Paraphotons

Chameleons

Light-Shining-through-Wall experiments

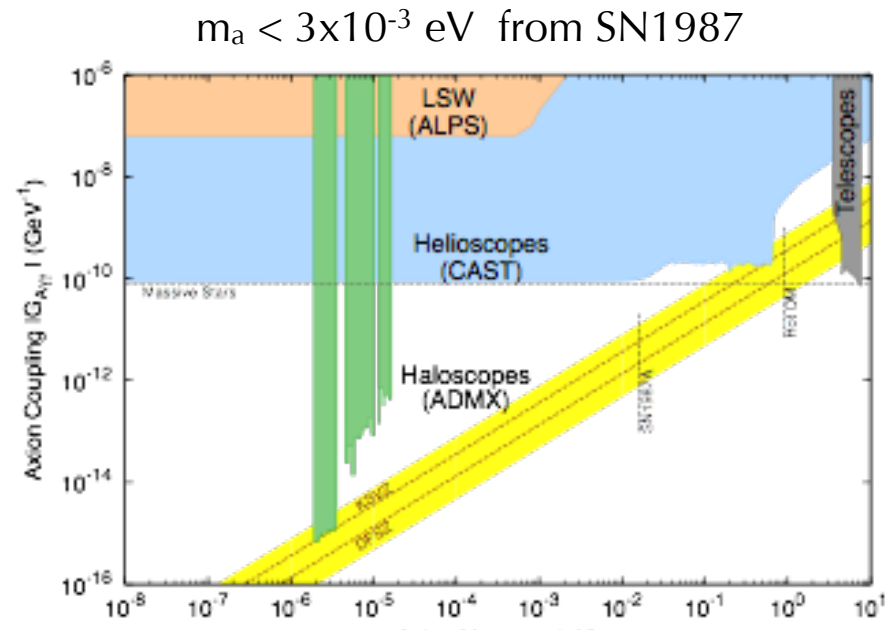
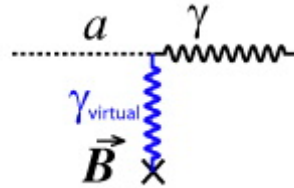
Presented at ICHEP16

Axions Experiments



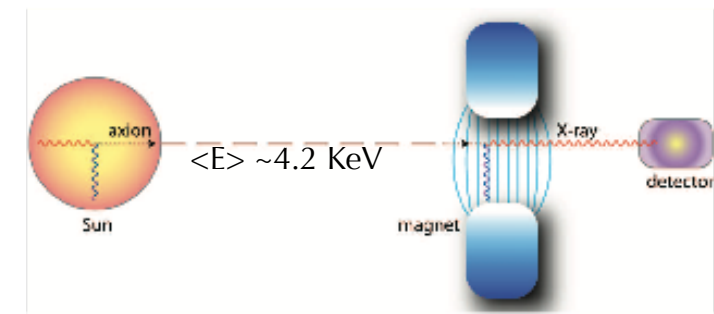
3 classes of experiments: Haloscopic, Helioscopic, LSW

Axion, like neutral pion couples to two photons via Primakoff effect
Detected in a magnetic field H

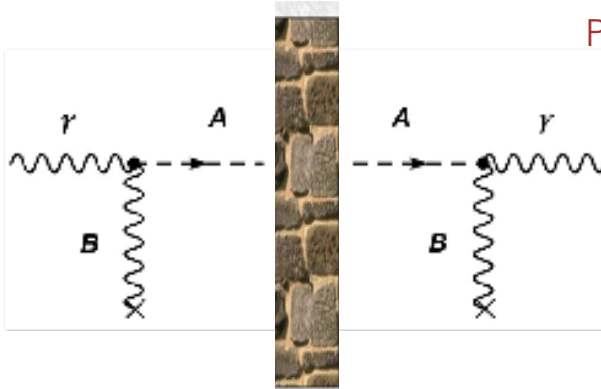


Yellow band represent theoretical predictions from DFSZ and KSVZ axion models

Haloscopic: cavity
Helioscopic depend on stellar models
CAST (best limit at the moment) and
IAXO (next CERN exp.) use LHC dipoles



Light Shining through a Wall Experiments



P. Sikivie, Phys. Rev. Lett. **51**, 1415 (1983)

LAB experiment
Laser Source
Higher Luminosity

Double process
Rate $\sim G^4$

$$\dot{N}_{\text{evts}} \propto \dot{N}_\gamma P_{\gamma \rightarrow a} \times P_{a \rightarrow \gamma} \sim \dot{N}_\gamma G^4 H^4 L^4$$

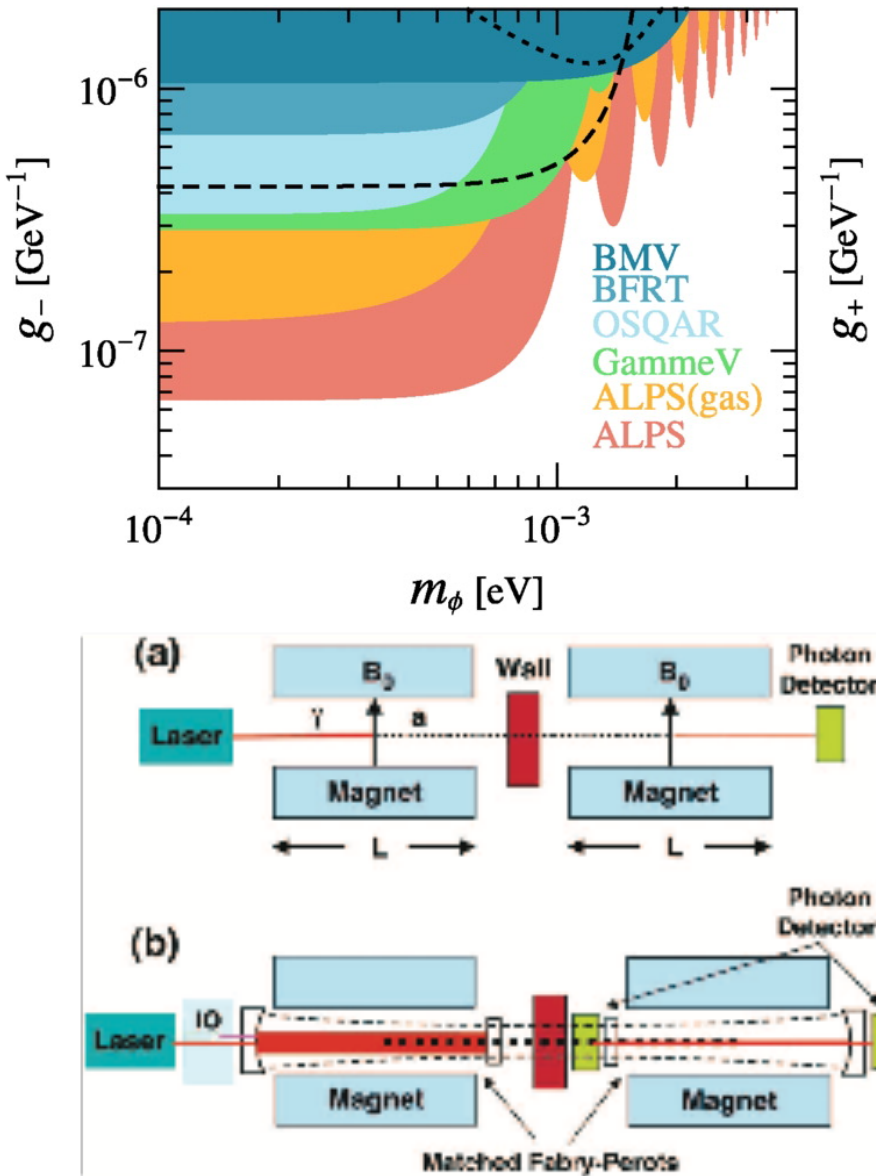
Sensitivity on G linear with L and H , quartic root of luminosity (not depending on E_γ)

The STAX key points are:

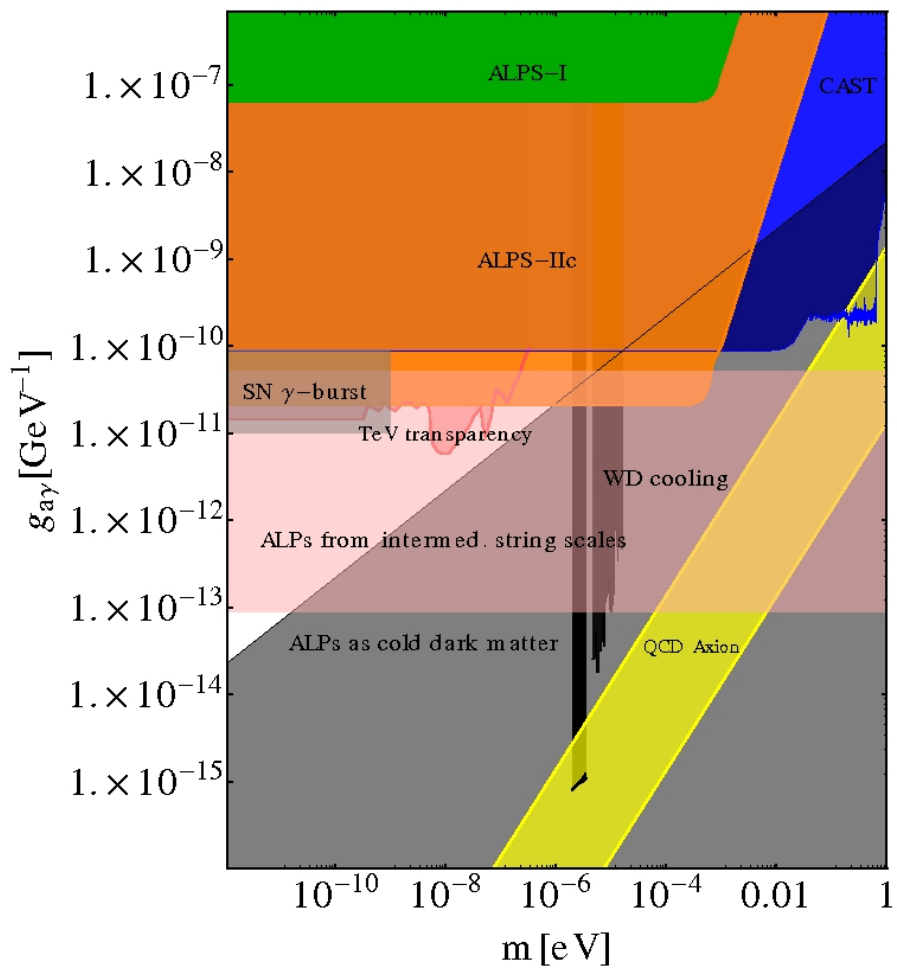
- High Luminosity (gyrotrons in the SubTHz region)
- intense $H \sim 15$ Tesla with $L \sim 50$ cm dipole
- Sub-THz single photon detector using TES

Optimal Working Point ~ 30 GHz

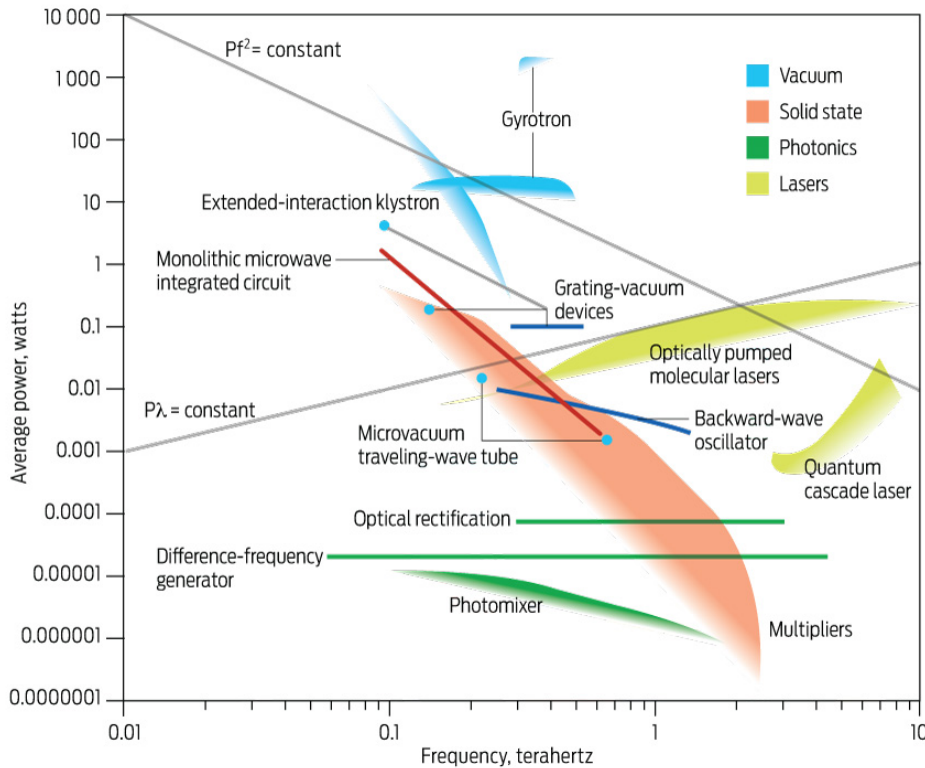
Light Shining through a Wall Experiments: ALPS



Ex: **ALPS** Desy use the Hera dipoles
 $N \sim 10^{19}$ photons/s



High Luminosity Photon Sources

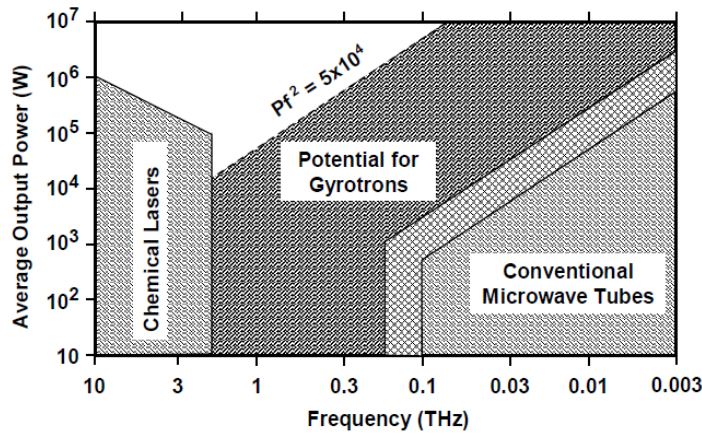


photon-axion conversion probability
depends on luminosity, not energy
⇒ sub-THz

Reference:
30 GHz \sim 120 $\mu\text{eV} \sim 1 \text{ cm}$

- Klystrons and gyrotrons sources in the 30-100 GHz range.
- Power exceeding 1 MW in this frequency range
- Luminosity up to 10^{28} - $10^{29} \gamma/\text{s}$ in CW
- Lasers commonly used in LSW experiments $\sim 10^{19} \gamma/\text{s}$

Gyrotrons



The operating region of gyrotrons

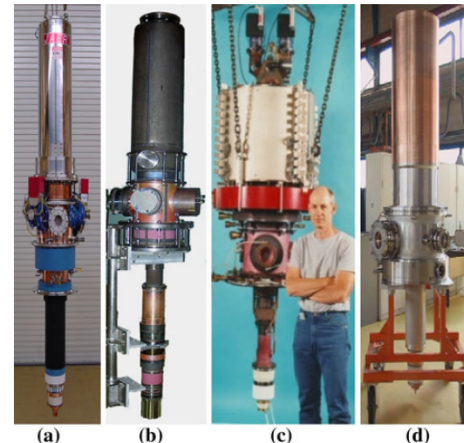
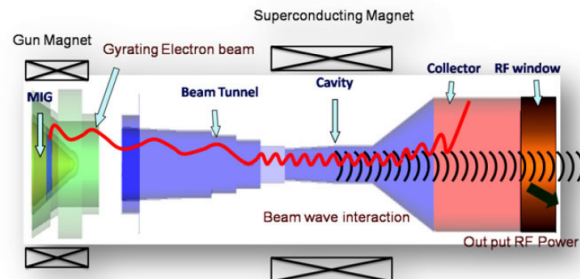
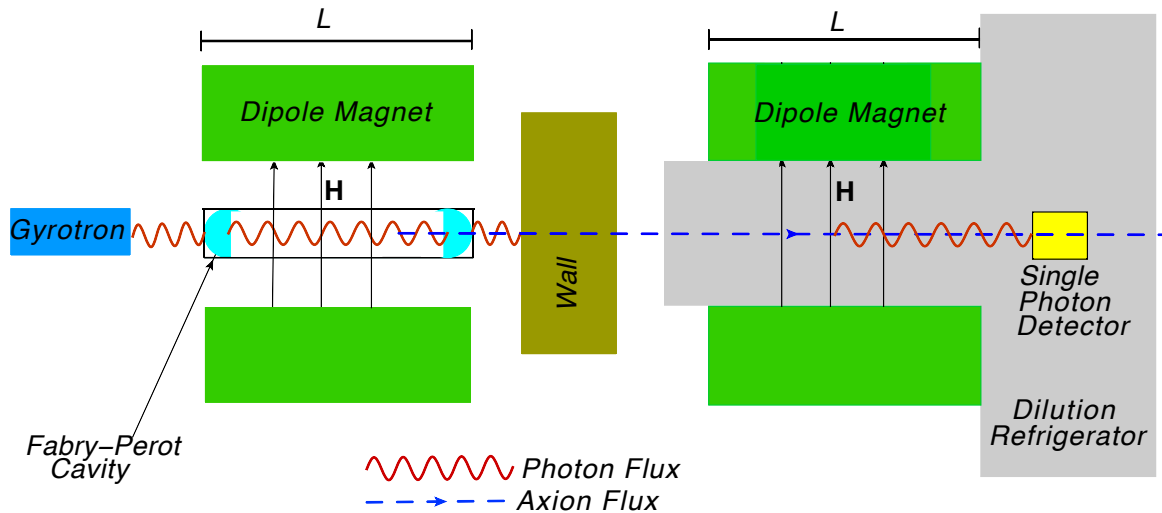


Fig. 2 Typical high power gyrotrons a JAERI/TOSHIBA 0.82 MW, 170 GHz, b GYCOM 1 MW, 170 GHz, c CPI 0.9 MW, 140 GHz, d TED 0.9 MW, 140 GHz



Now beyond 1 MW power

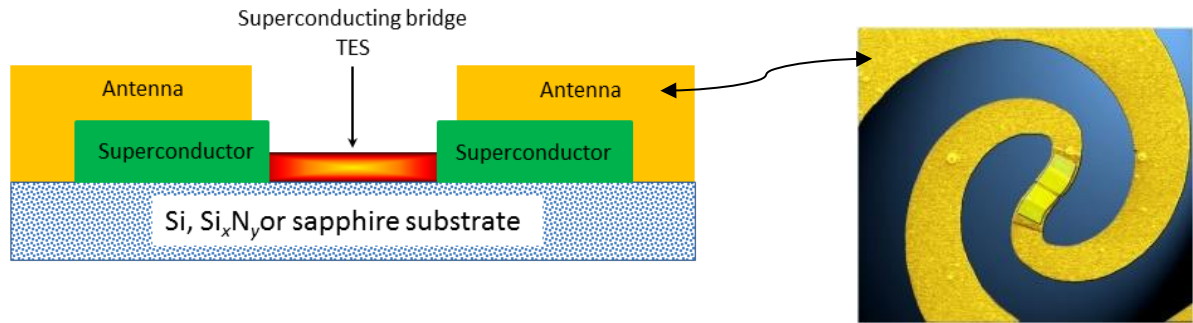
STAX Experiment



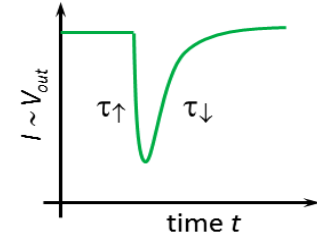
- Magnetic field: $H = 15 \text{ T}$, $L = 0.5 \text{ m}$
- Source: gyrotron; $P \approx 100 \text{ kW}$, $\Phi_\gamma = 10^{27} \text{ s}^{-1}$, $\varepsilon_\gamma = 120 \mu\text{eV}$ ($\nu \approx 30 \text{ GHz}$)
- Fabry-Perot cavity: $Q \approx 10^4$
- Sub-THz single-photon detection based on TES technology, $\eta \approx 1$
- Possible second FP cavity behind the wall to enhance axion-photon conversion rate

P. Sikivie, D.B. Tanner and K. Van Bibber, Phys. Rev. Lett. 98, 172002 (2007)

STAX detector



- Sub-THz single photon detector
- Transition Edge Sensor **TES**: ultra-low critical temperature superconductor bridge between two superconducting electrodes. TES coupled to a log periodic antenna.
- TES operates within its superconducting transition. DC bias voltage applied. When TES absorbs an incoming photon, it heats up above critical temperature Tc. Change of resistance and current flowing in the circuit, measured by a SQUID
- Material: choice of a Superconductor with low critical temperature ($T_c \approx 20$ mK) to have a good energy resolution α -W or bilayer Ti-Au or Ti-Cu
- TES bridge Ti-Cu (gap ~ 20 μ eV), superconducting electrodes Nb (gap ~ 1 meV)
- Very high efficiency
- Ultra low background/dark count



STAX detector

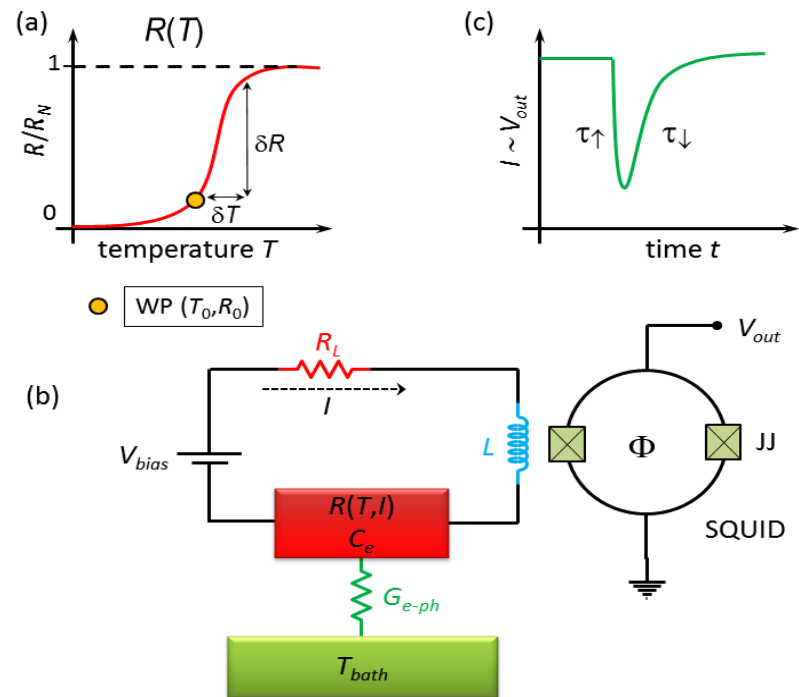
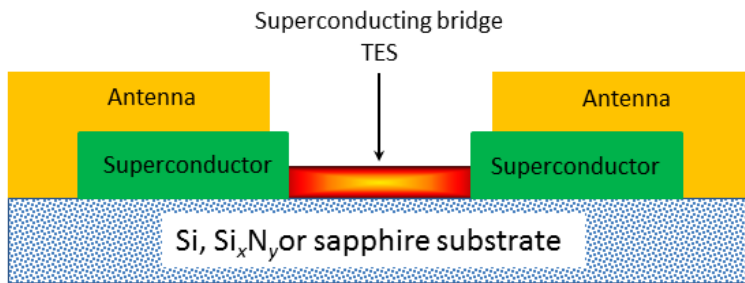


- Tailoring TES active **volume** to reduce thermal capacitance (10^{-3} - $10^{-4} \mu\text{m}^3$)

$$\sigma_E \approx 0.3\sqrt{k_B T_c^2 C_e}$$

$$C = \gamma V T \quad V \sim 300 \times 40 \times 20 \text{ nm}^3$$

- low-noise SQUID readout electronics optimization (operating at 80 mK)
- Sensitivity $\delta T = \delta E / C_e$ thermalization $T(t) = \exp(-t/\tau)$ $\tau = C_e / G$



Noise



- Dark count rate (phonon noise) $< 6 \times 10^{-10} \text{ s}^{-1}$
- Black Body: at 10mK peaked around 0.6 GHz with a negligible rate of $10^{-30} \text{ m}^{-2} \text{ s}^{-1}$ photons irradiated
- Cosmic bkg: $1 \mu\text{cm}^{-2}/\text{min}$ with 10 eV released in 10nm of material saturates the TES, bkg. under control translated in a negligible dead time of the TES $\sim 0.1\%$

$$N_d = \frac{\beta_{\text{eff}}}{\sqrt{2\pi}} \int_{E_T/\sigma_E}^{\infty} \exp(-x^2/2) dx.$$

where $\beta_{\text{eff}} = 1/\tau_{\text{eff}}$ is the effective detection bandwidth, and E_T is the discrimination threshold energy.

$$\eta = \frac{1}{\sqrt{2\pi}} \int_{(E_T - h\nu)/\sigma_E}^{\infty} \exp(-x^2/2) dx.$$

Scheme of the temperatures in the experimental dilution cryostat set-up

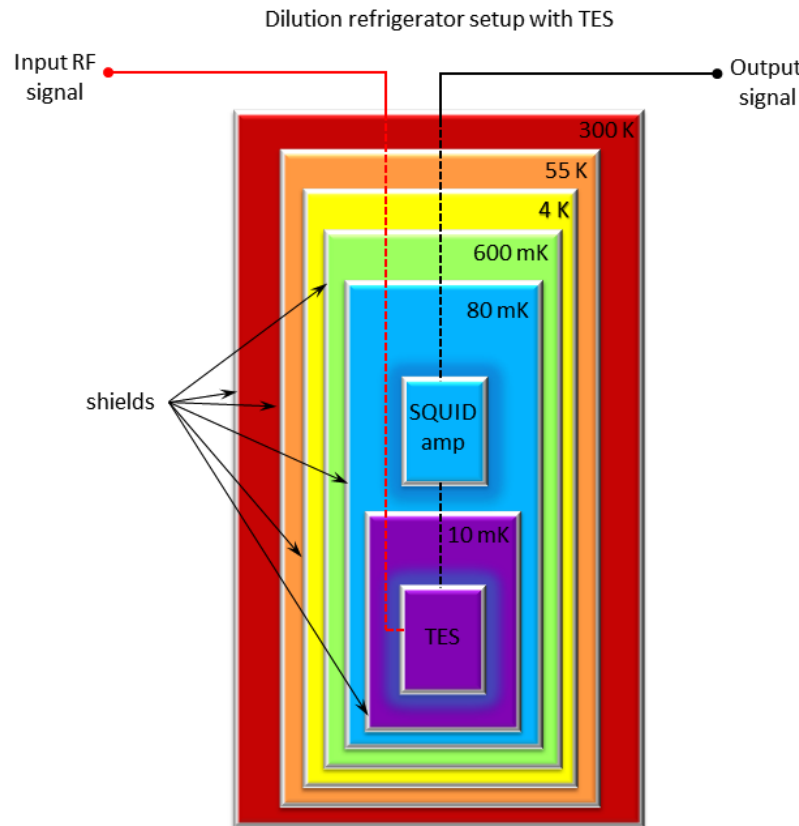


Figure 8 Scheme of the experimental setup of the TES based on a dilution refrigerator. The cryostat metallic shields reside at different temperatures from 300 K to below ~ 10 mK. The enclosure containing the TES element is at the fridge base temperature whereas the readout SQUID amplifier is kept at 80 mK to improve its noise performance. Input microwave radiation is fed into the fridge, and thereby into the TES detector, via coaxial cables while the low-frequency output signal coming from the SQUID is read via conventional DC lines.

Alternative choices to boost the experiment



- Work with a new concept Fabry Perot to enhance the Q factor
- An upgrade in Q translates into the need of a lower power of the source P/Q^2

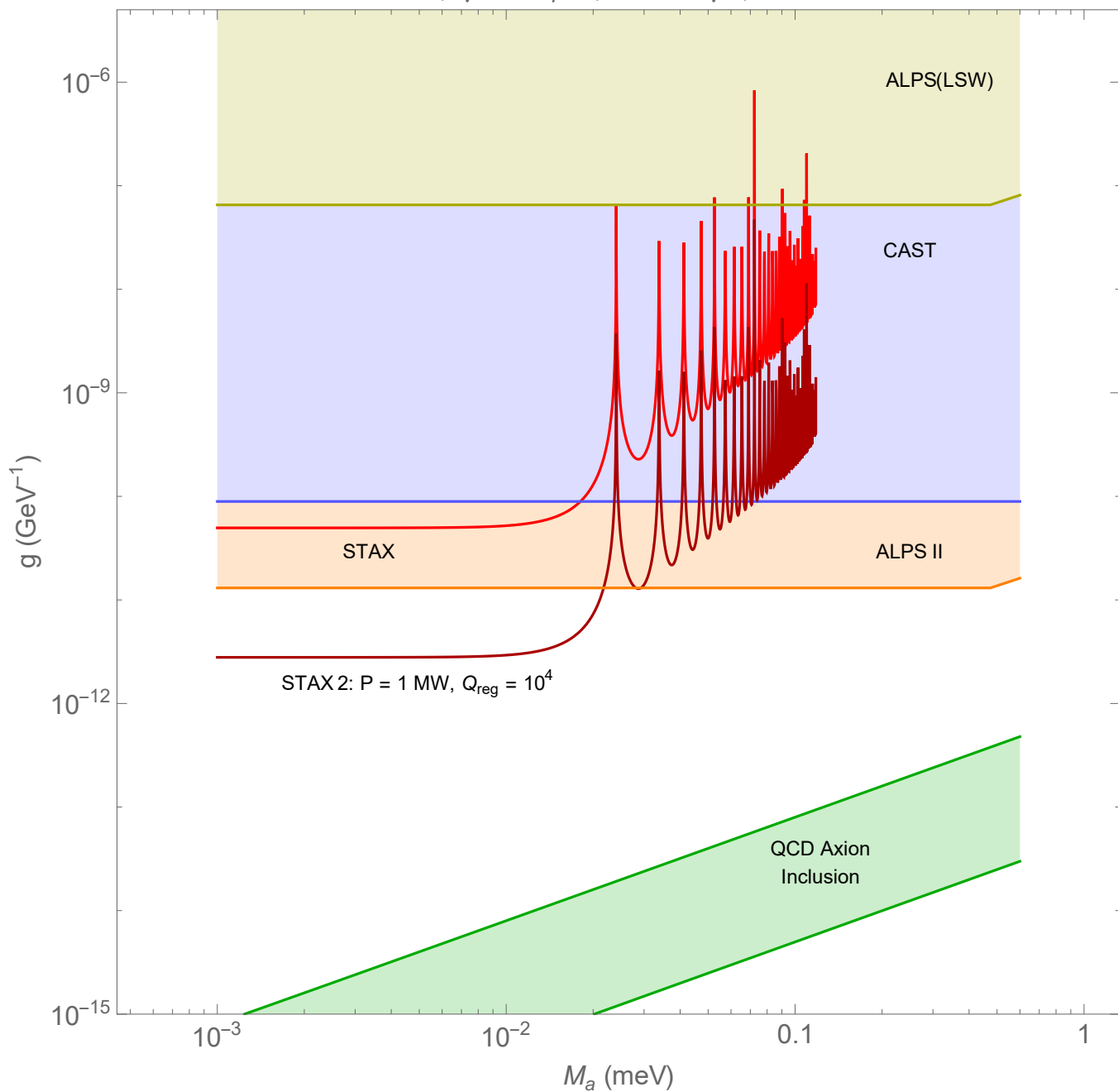
$$\dot{N}_{\text{evts}} \propto \dot{N}_\gamma P_{\gamma \rightarrow a} \times P_{a \rightarrow \gamma} \times Q^2$$

- Fabry Perot with Q exceeding 10^{10} have been recently developed with superconducting cavities
- Material choice need to be shaped to work in this particular environment
 - Low temp
 - High B field
- High Q and lower P can drive the use of other (more refined and easier to handle) photon sources than gyrotrons (klystrons?)
- or also to a lighter B fields (split coil vs solenoid?)

$$P_{\gamma \rightleftharpoons a} = g^2 H^2 \frac{\sin^2 \left(\frac{q_x L_x}{2} \right)}{q_x^2}$$

$$q_x = \frac{m_a^2}{2\mathcal{E}_\gamma}$$

Exclusion Plot Axion-Like Particle.
 STAX: Time: $2.6 \cdot 10^6$ s, H = 15 T, Lx = 0.5 m
 $Q = 10^4$, $E\gamma = 118 \mu\text{eV}$, $\dot{N} = 10^{27} \text{ g/s}$, P = 100 kW

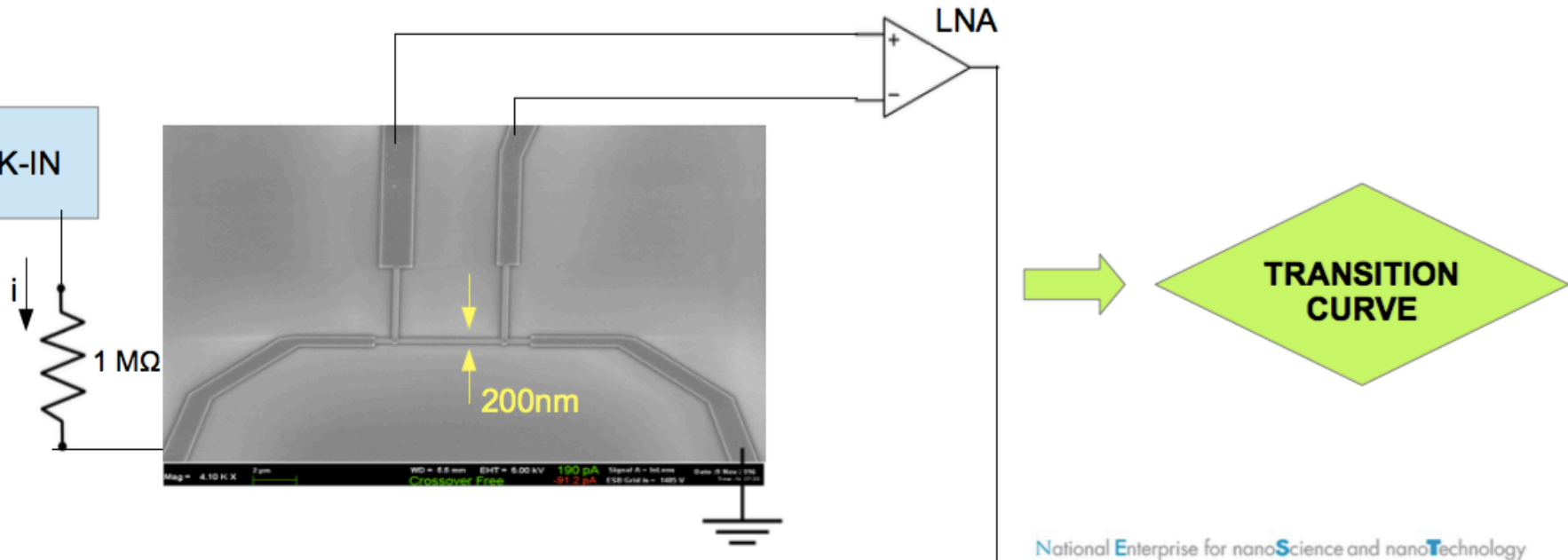




| Parameter | ALPS | STAX | g_{ALPS} / g_{STAX} | STAX II | g_{ALPS} / g_{STAXII} |
|-----------------------------|--------------------------------------|----------------------------|-----------------------|----------------------------|-------------------------|
| Laser Power | 0.8 W | 100 kW | 18.8 | 1 MW | 188 |
| Photon Energy | 2.327 eV | 124 μ eV | 11.7 | 124 μ eV | 11.7 |
| Cavity Q-factor | 55.0 | 10^4 | 3.7 | 10^8 | 37 |
| H * L_x | 22 T m | 7.5 T m | 0.3 | 7.5 T m | 0.3 |
| Detection Efficiency | 0.9 | 1.0 | 1.0 | 1.0 | 1.0 |
| Detector Noise | $1.8 \cdot 10^{-3} \text{ sec}^{-1}$ | 10^{-9} sec^{-1} | 34.0 | 10^{-9} sec^{-1} | 34 |
| Combined Improvement | | | $\sim 10^4$ | | $\sim 8 \times 10^5$ |



- Cu/Al and Cu/Ti bilayers designed as **5 µm X 200 nm strip** of different total thickness and thickness ratio
 - Fabrication via e-beam lithography + e-beam evaporation
 - 4-wires measurements of the resistance using a lock-in circuit



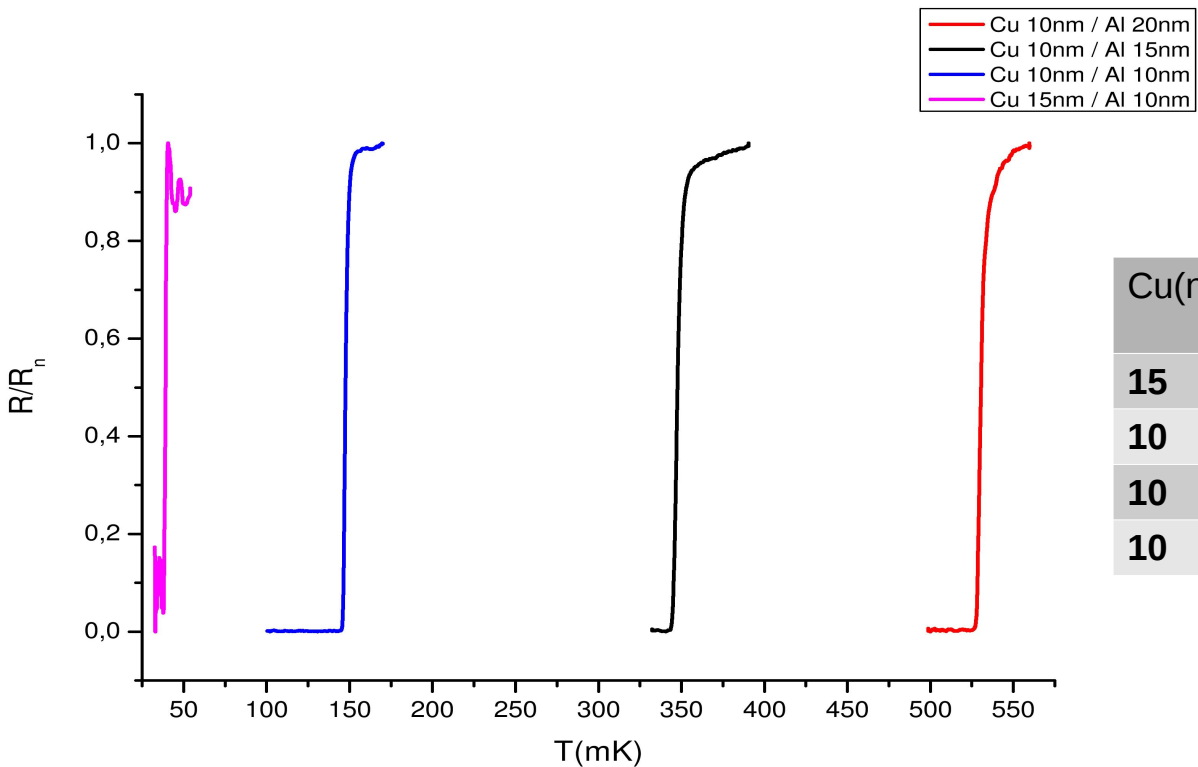
Yuri Venturini

National Enterprise for nanoScience and nanoTechnology

NFEST



T_c of Cu/Al bilayers



$$\alpha = \text{MAX}(T/R \cdot dR/dT)$$

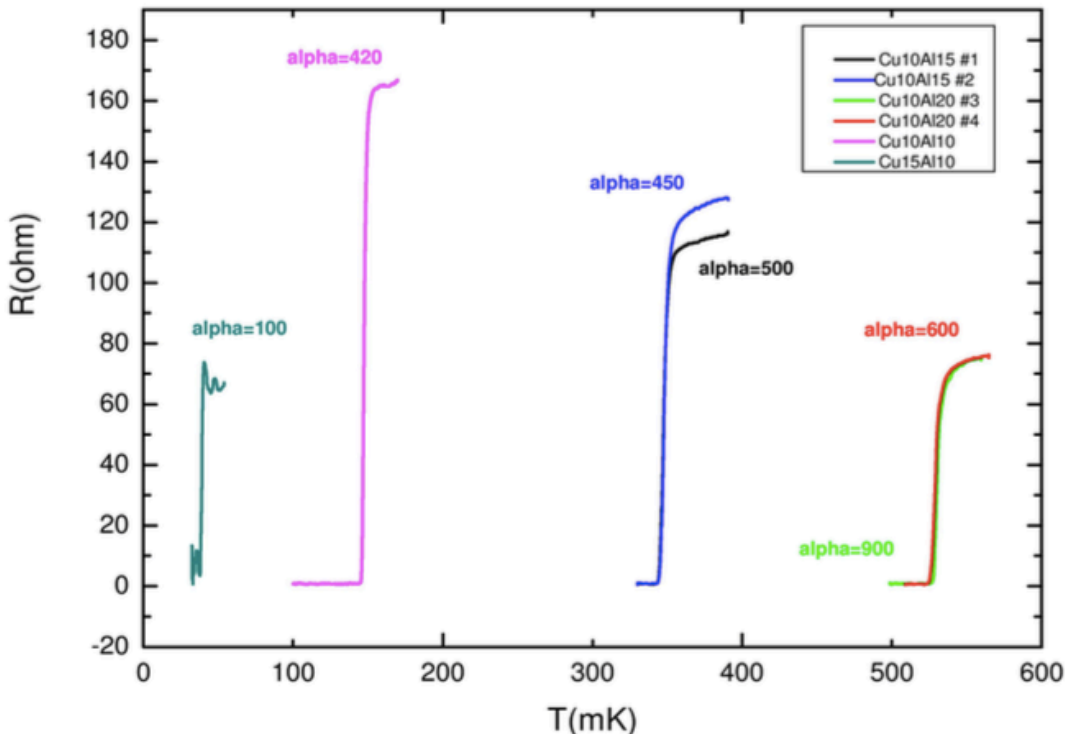
| Cu(nm) | Al(nm) | T _c (mK) | R _n (ohm) | alpha |
|--------|--------|---------------------|----------------------|-------|
| 15 | 10 | 40 | 70 | 100 |
| 10 | 10 | 147 | 165 | 420 |
| 10 | 15 | 347 | 115 | 500 |
| 10 | 20 | 530 | 75 | 900 |

national Enterprise for nanoScience and nanoTechnology

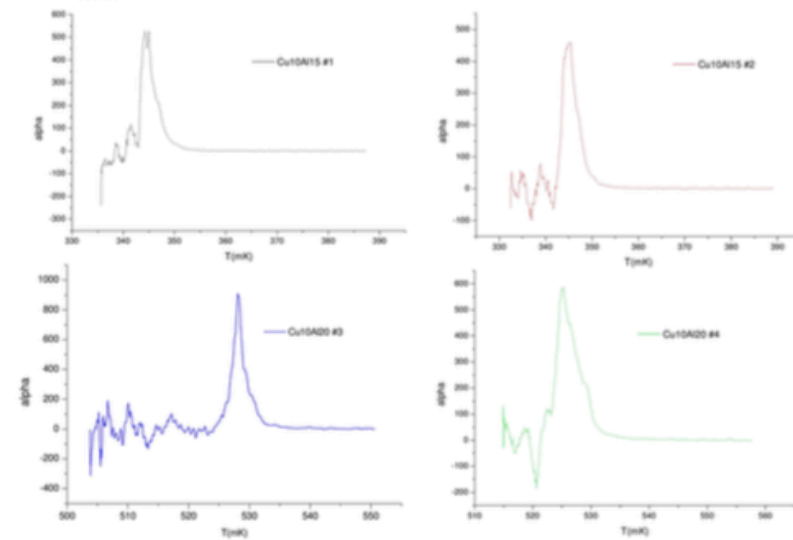


T_c of Cu/Al bilayers (1)

all transitions are measured with a lock-in circuit with input current $i = 6\text{nA}$, except for Cu15Al10 ($i=0.1\text{nA}$)



Data analysis: extraction of $\alpha = T/R \cdot dR/dT$



In the plot are reported the thicknesses and the max value of alpha

National Enterprise for nanoScience and nanoTechnology



Next Steps...



- Cu/Ti up down to $T_c \sim 20\text{mK}$
- Coupling with a SQUID read-out
- Test with a 30 GHz photon source
- R&D of the Fabry Perot
- Design of the log periodic antenna
- R&D of the Fabry Perot
- Magnet design



BACK UP SLIDES

BACK-UP

- Wavelength associated to virtual axion $\lambda = 1/p_x \approx L_x$
 Uncertainty principle: $\Delta x \approx L_x \rightarrow \Delta p \geq 1/L_x$
 In more details, if $\lambda/2 < L_x$ the entire process takes place in the $H \neq 0$ region
- Consider $\epsilon_\gamma \neq m_a$, so that $q_1 \geq m_a + 1/2L$, $q_2 \leq m_a - 1/2L$
 Poles coincide when $\epsilon_\gamma = m_a$ ($p^* = 0$)
 Minimum distance between poles must satisfy: $\min(q_1 - q_2) = 1/L$
- We argue the formula

$$P_{\gamma \rightarrow a} \approx G^2 H^2 \frac{\sin^2(q_x L_x / 2)}{q_x^2} \frac{\epsilon_\gamma}{\frac{1}{L_x} + \sqrt{\epsilon_\gamma^2 - m_a^2}}$$

to be used when $\epsilon_\gamma \approx m_a$ to avoid unphysical divergences

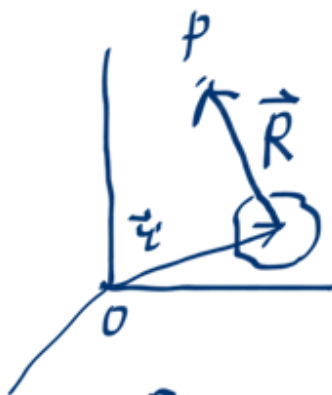
Axion-like particles

$$\mathcal{L}_T = \frac{1}{4} a F_{\mu\nu} \tilde{F}^{\mu\nu}$$

$$\tilde{F}^{\mu\nu} = \frac{1}{2} \epsilon^{\mu\nu\rho\sigma} F_{\rho\sigma}$$

$$\square a = \frac{1}{M} \vec{H}^{\text{ext}} \cdot \frac{\partial}{\partial t} \vec{A} - m^2 a$$

Cfr. Poisson eq. in electricity:

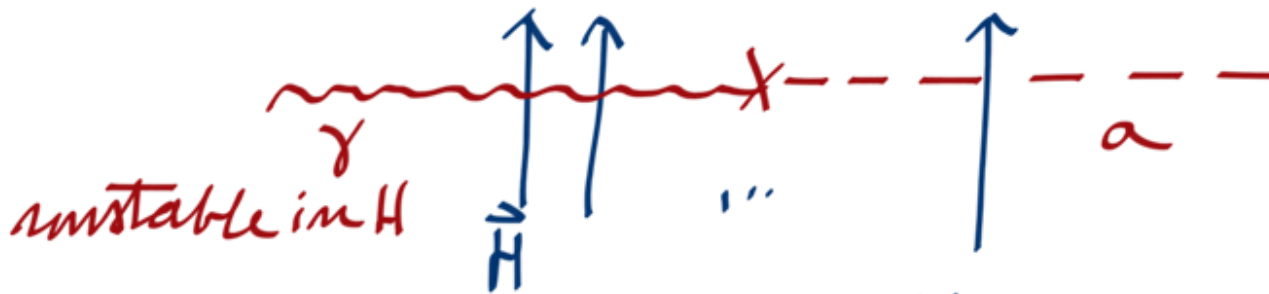


$$\Delta \phi + k^2 \phi = -4\pi \rho$$

$$\phi = \int \rho(\vec{r}', t - \frac{R}{c}) \frac{e^{ikR}}{R} dV'$$

$$R \approx r - \vec{r}' \cdot \hat{m}' \quad \vec{k}' = k \hat{m}' \quad n \gg n'$$

Photon - Axion Conversion



$$a = f \frac{e^{ik_r}}{r}$$

$$\boxed{\left| M_{\gamma \rightarrow a} \right|^2 = \frac{1}{4\pi^2} \left| \int e^{i\vec{q} \cdot \vec{r}} \vec{H}(\vec{r}) \cdot \vec{E}(\vec{k}_\gamma, \chi) dV \right|^2}$$

Max when $\vec{k}_\gamma \perp \vec{H}$

Formula holds for $\epsilon_\gamma = \epsilon_a$

Notice $|\vec{k}_\gamma| \neq |\vec{k}_a|$ and $\vec{q} = \vec{k}_\gamma - \vec{k}_a$

Conversion Probability

In the \perp plane H extends over long dist. wrt $1/q_y \approx 1/q_z$ - In the \parallel direction we assume $L_x \lesssim 1/q_x$.

$$P_{\text{conversion}} = \frac{H^2}{M^2} \frac{\sin^2\left(\frac{q_x L_x}{2}\right)}{q_x^2} \left(\frac{\epsilon_y}{|k_a|}\right)$$

$$q_x = \frac{m_a^2}{2\epsilon_y}$$

$$|\vec{k}_a| = \sqrt{\epsilon_y^2 - m_a^2} = \sqrt{\epsilon_y^2 - m_a^2} \sim \epsilon_y \text{ as } \epsilon_y \gg m_a$$

Dark photons

L.B. Okun, Sov. Phys.-JETP **56**, 502 (1982)

B. Holdom, Phys. Lett. B **166**, 196 (1986)

- Massive vectors of hidden $U(1)_h$
- Visible and hidden-sector photons Lagrangian:

$$\mathcal{L} = -\frac{1}{4}F^{\mu\nu}F_{\mu\nu} - \frac{1}{4}B^{\mu\nu}B_{\mu\nu} + eJ_{\text{em}}^\mu A_\mu + e_h J_h^\mu B_\mu - \frac{1}{2}\mu^2 B^\mu B_\mu$$

$F^{\mu\nu}$ = field strength tensor for A^μ ; $B^{\mu\nu}$ = field strength tensor for B^μ (paraphoton)

- \mathbf{A} and \mathbf{B} rotated into \mathbf{B}_1 and \mathbf{B}_2 ; mixing angle $\chi < 10^{-2}$
 \mathbf{B}_1 and \mathbf{B}_2 acquire masses $m_1 = \mu\chi$, $m_2 = \mu$

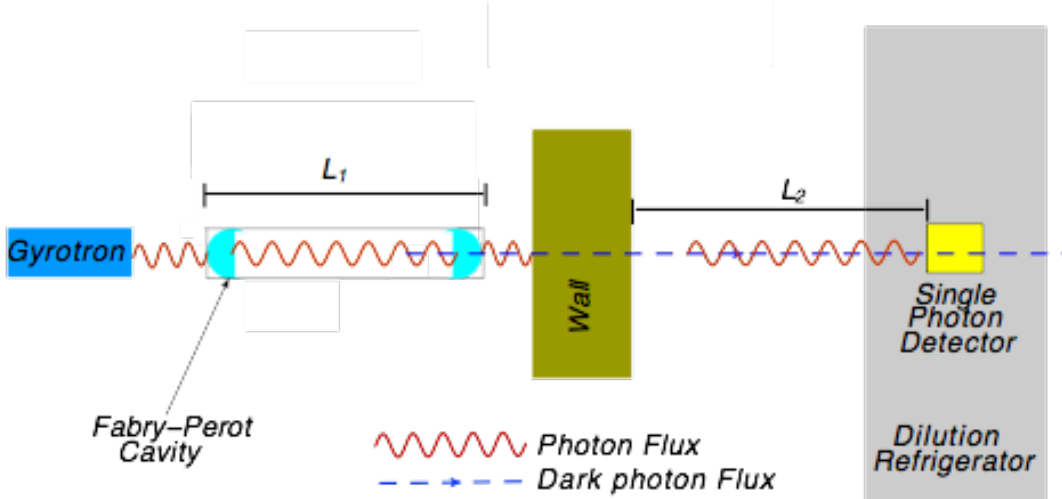
- Photon field evolve as:

$$A(r) = \frac{1}{\chi^2 + 1} e^{-i(\epsilon_\gamma t - k_1 r)} [A(1 + \chi^2 e^{-iqr}) + \chi B(e^{-iqr} - 1)]$$
$$k_1 \approx \epsilon_\gamma$$
$$k_2 \approx \sqrt{\epsilon_\gamma^2 - \mu^2}$$
$$q = k_1 - k_2$$

Dark photons

L.B. Okun, Sov. Phys.-JETP **56**, 502 (1982)

B. Holdom, Phys. Lett. B **166**, 196 (1986)

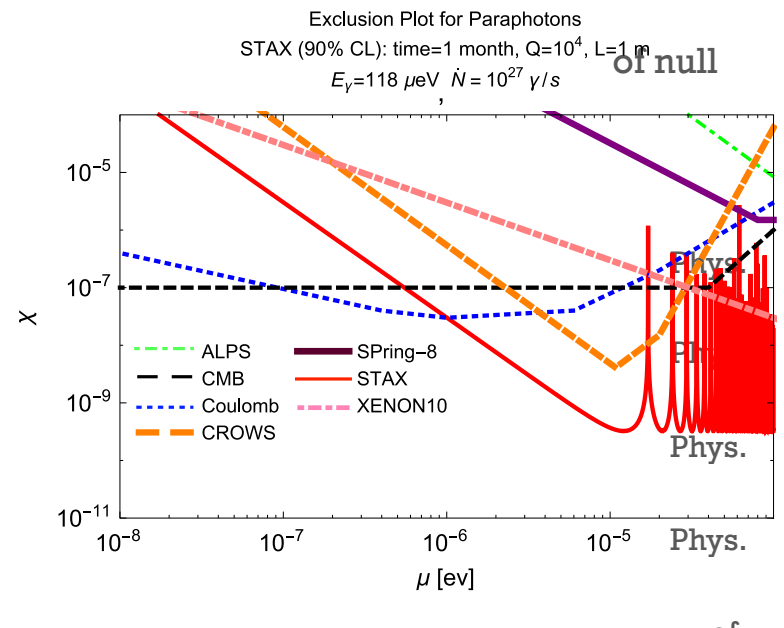


- Conversion probability: $P_{\gamma \rightarrow \gamma'}(r) = 4\chi^2 \sin^2\left(\frac{qr}{2}\right)$
$$P_{\gamma \rightarrow \gamma' \rightarrow \gamma} = P_{\gamma \rightarrow \gamma'}(L_1)P_{\gamma' \rightarrow \gamma}(L_2)$$
$$= 16\chi^4 \left[\sin\left(\frac{qL_1}{2}\right) \sin\left(\frac{qL_2}{2}\right) \right]^2$$
- Rate: $\frac{dN_\gamma}{dt} = \eta \Phi_\gamma \left[\frac{N_{\text{pass}} + 1}{2} \right] P_{\gamma \rightarrow \gamma' \rightarrow \gamma}$ Φ_γ = photon flux (s^{-1}), η = detector efficiency

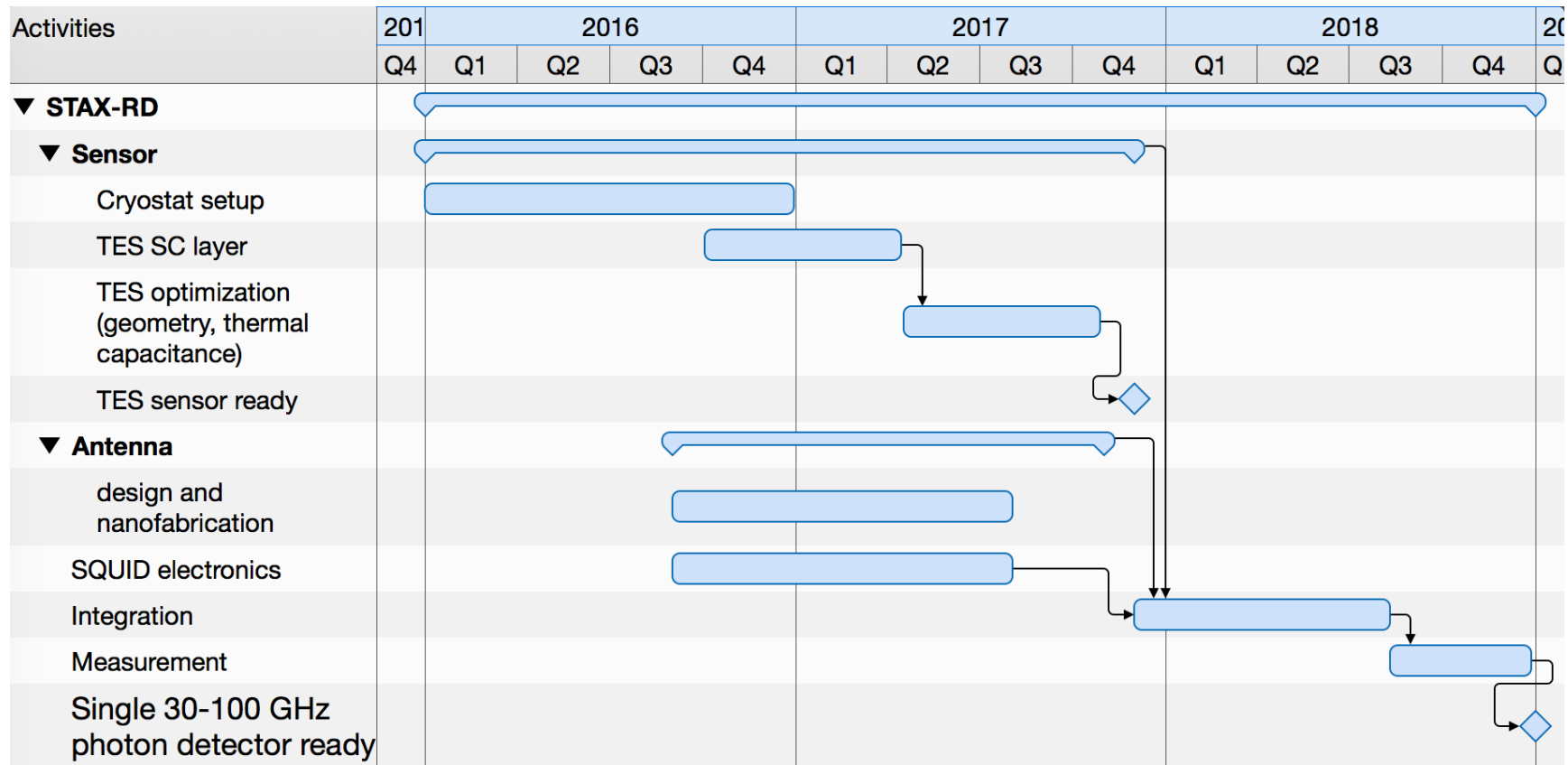
Search for dark photons at STAX

L.M. Capparelli *et al.*, Phys. Dark Univ. **12**, 37 (2016)

- Exclusion limits STAX may achieve in case result
- **STAX** limits compared to
 - **ALPS LSW** results
Lett. B **689**, 149 (2010)
 - **CROWS** results
Rev. D **88**, 075014 (2013)
 - **Spring-8** results
Lett. B **722**, 301 (2013)
 - **XENON10** results
Lett. B **689**, 149 (2010)
 - Constraints on dark photons from measurements the **CMB**
Astrophys. J. **473**, 576 (1996)
 - Searches for modifications of **Coulomb's Law**
Phys. Rev. Lett. **61**, 2285 (1988)



3 years R&D project



Facilities located between INFN-Pisa and NEST-Pisa
possibility to use INFN S.Piero Labs

Financial Plan and Requests

| Description | Quantity | Unit Price | Cost |
|--|----------|------------|-----------------|
| cryogen-free dilution refrigerator | 1 | €200.000 | €200.000 |
| SQUID amplifiers | 2 | € 20.000 | € 40.000 |
| mw Gunn oscillator radiation sources | 3 | € 30.000 | € 90.000 |
| vector network analyser | 1 | €100.000 | €100.000 |
| mw NbTi superconducting coaxial cables | 6 | € 2.000 | € 12.000 |
| 10 Tb disk storage | 1 | € 3.000 | € 3.000 |
| CPU (HS06 units) | 500 | € 12 | € 6.000 |
| Consumables per year | 3 | € 15.000 | € 45.000 |
| travel cost per year | 3 | € 15.000 | € 45.000 |
| publication cost per year | 3 | € 4.000 | € 12.000 |
| personnel per year | 6 | € 30.000 | €180.000 |
| Total | | | €733.000 |

Financial Plan and Requests

| Description | 2016 | 2017 | 2018 | Total |
|------------------------------------|------------------|------------------|------------------|------------------|
| cryogen-free dilution refrigerator | €200.000 | | | €200.000 |
| SQUID amplifiers | | € 20.000 | € 20.000 | € 40.000 |
| radiation sources | | €90.000 | | € 90.000 |
| vector analyser | | | €100.000 | €100.000 |
| superconducting coaxial cables | € 12.000 | | | € 12.000 |
| Storage | | € 3.000 | | € 3.000 |
| CPU | | € 6.000 | | € 6.000 |
| Consumables | € 15.000 | € 15.000 | € 15.000 | € 45.000 |
| travel cost | € 15.000 | € 15.000 | € 15.000 | € 45.000 |
| publication cost | | € 6.000 | € 6.000 | € 12.000 |
| personnel | € 60.000 | € 60.000 | € 60.000 | €180.000 |
| Total | 302.000 € | 215.000 € | 216.000 € | 733.000 € |